

Synthesis of Biodiesel by Nanoporous Catalysts Supported Alkali Metals and its Hydroxides

Dr. Talib M. Albayati 

Chemical Engineering Department, University of Technology/ Baghdad

Email: talib_albyati@yahoo.com

Aidan M. Doyle²

Division of Chemistry and Environmental Science, Manchester Metropolitan University, Chester St., Manchester, M1 5GD, United Kingdom.

ABSTRACTS

The alkali metals make up first group of the periodic table. This family consists of the elements lithium, sodium, potassium, rubidium, cesium, and francium (Li, Na, K, Rb, Cs, and Fr, respectively).

The influence of alkali metals and its hydroxides supported on catalysts prepared SBA-15 for the synthesis of agro or biodiesel fuels from vegetable oil were investigated via heterogeneous catalytic reaction. The structural and textural features encapsulated Nanoporous Material SBA-15 were studied by X-ray diffraction, scanning electron microscopy (SEM), EDAX, nitrogen adsorption-desorption (BET) and FTIR characterization were also carried out on the catalysts before and after loading. Mild conditions (atmospheric pressure and 65 °C) were chosen for catalytic activity reaction testing in a batch reactor. The results show that all the catalysts were found active for the esterification reaction of vegetable oil conversion around (85-94%).

This study shows that the alkali metals and its hydroxides supported catalysts on SBA-15 based catalyst have proven to be a promising one for the transesterification of vegetable oil with methanol.

Keywords: Esterification reaction, Biodiesels, SBA-15, alkali metal, alkali Hydroxide.

انتاج وقود الحيوي باستخدام العوامل المساعدة النانوية المسامية المحملة على المعادن واكاسيدها المائية

الخلاصة

تشكل الفلزات القلوية المجموعة الاولى من الجدول الدوري. تتكون هذه العائلة من العناصر الليثيوم (Li)، الصوديوم (Na)، البوتاسيوم (K)، الروبيديوم (Rb)، السيزيوم (Cs)، والفرانسيوم (Fr) على الترتيب. ان تأثير الفلزات القلوية وهيدروكسيداتها المحملة على العامل المحفز (العامل المساعد) SBA-15 لصناعة وقود الديزل الحيوي من الزيوت النباتية تم دراستها عن طريق التفاعل المحفز الغير المتجانس. ان تركيب المادة ومميزات السطح الخارجي للمادة النانوية المسامية تم دراستها قبل وبعد التحميل. بواسطة

الاشعة السينية XRD بالاضافة الى دراسة المسح الالكتروني المجهر SEM وتحليل نسبة العناصر EDAX. وكما تم قياس المساحة السطحية وقطر المسامات بواسطة غاز النيتروجين بعملية الامتزاز وازالة الامتزاز BET. بالاضافة الى قياس المجاميع الفعالة بواسطة FT-IR. وقد تم اختيار ظروف معتدلة لعملية التشغيل (عند الضغط الجوي ودرجة حرارة 65 مئوي) لدراسة فعالية العامل المساعد. وظهرت النتائج التي تم الحصول عليها في جميع انواع العوامل الحفازة التي اختبرت في تفاعل الاسترة بان تحويل الزيت النباتي الى البايوديزل او الوقود الحيوي كان بحدود (85-94%). وتبين هذه الدراسة أن الفلزات القلوية وهيدروكسيداتها المحملة كمحفزات على المادة النانوية المسامية SBA-15 قد اثبتتكون واحدة من العوامل المحفزة الجيدة لتفاعلات الاسترة لانتاج الوقود الحيوي من تفاعل الزيوت النباتية مع الميثانول.

INTRODUCTION

In the near future scenario, the project of renewable alternate fuels sources will be of increasing importance; for example agro or biodiesel fuels, which are fuel grade derivate of vegetable oils. Today's most important source of energy and chemicals is crude oil and consumption of this resource enhances everyday as countries develop. The International Energy Agency (IEA) foresees that fossil fuels will continue to dominate energy supplies in 2030 with the transportation sector expected to account for two-thirds of the growth, and global daily oil demand will possibly reach 115 million barrels per day in 2030[1]. However, this would strongly diminish the reserved crude oil resources, and result in the increase in the price of petroleum. Additionally, as this energy resource is not renewable, emission of CO₂ and other particulates would increase greenhouse-gas effects [2–4].

Improvement of biodiesel composition is a huge challenge because of the importance of its positive impact on the environment [5–7]. Biodiesel is an alternative to fossil fuels allowing a reduction in CO₂ emission [8, 9].

Biodiesel is a renewable liquid fuel, derived from triglycerides holds promise to compensate the increase demand of petroleum diesel [10]. The process of transesterification of triglyceride with methanol, ethanol or any other suitable alcohol produces biodiesel [11–13]. Transesterification, also called alcoholysis, is the reaction of an oil or fat with an alcohol to form esters and glycerol. The basic reaction is depicted in Figure (1).

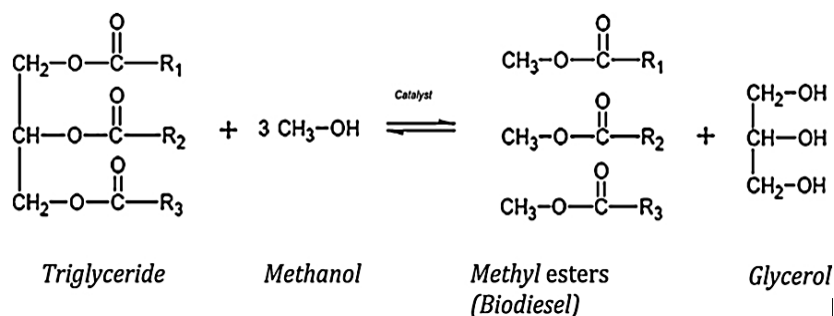


Figure (1) Typical Tran's esterification reaction of a triglyceride with methanol [14].

The reaction is facilitated with a suitable catalyst [15]. If the catalyst remains in the same (liquid) phase to that of the reactants during transesterification, it is homogeneous catalytic transesterification. On the other hand, if the catalyst remains in different phase (i.e. solid, immiscible liquid or gaseous) to that of the reactants the process is called heterogeneous catalytic transesterification [16, 17]. The heterogeneous catalytic transesterification is included under Green Technology due to the following attributes: (1) the catalyst can be recycled (reused), (2) there is no or very less amount of waste water produced during the process and (3) separation of biodiesel from glycerol is much easier [18,19]. During homogeneous catalytic transesterification the glycerol produced is of low quality and requires lengthy process and distillation for purification [20–23]. All these processing increases the cost of the end products: biodiesel and glycerin. Moreover, the homogeneous base catalyzed transesterification process encountered problems to handle multiple feed stocks. On the other hand, heterogeneous catalytic transesterification process overcomes these problems because methanol or ethanol does not mix with solid heterogeneous catalyst. After the transesterification reaction it is relatively easy to separate the catalyst from biodiesel and glycerol.

This study was conducted to synthesis highly ordered Nanoporous material SBA-15 catalysts encapsulated with alkali metals and its hydroxides in order to examine the role of their chemical composition on the heterogeneous base catalytic performance in production of biodiesel by esterification of vegetable oil.

EXPERIMENTAL

Chemicals

All chemicals viz. triblock copolymer poly (ethylene glycol) - Block-poly (Propylene glycol)-Block-poly (ethylene glycol) (Pluronic P123, Molecular weight=5800, EO20PO70EO20), tetraethylorthosilicate (TEOS), hydrochloric acid (HCl), LiOH, NaOH, Li₂CO₃ and Na₂CO₃ were purchased from Sigma Aldrich Chemical Inc. All chemicals were used as received without further purification. Millipore water was used in all experiments.

Preparation of Catalyst

Mesoporous silica SBA-15 was prepared using the conventional methods [24]. Syntheses were performed using triblock copolymer, poly (ethylene glycol)-block-poly (propylene glycol)-block-poly (ethylene glycol) (PEG-PPG-PEG), (6 g) Pluronic P123 (triblock co-polymer, EO20PO70EO20, MW=5800) as the structure directing agent and dissolved into deionized water (45 g) and 2 M HCl (180 g) while stirring at 35-40 °C for 30 min. After that tetraethylortho silicate (TEOS) as the silica source under acidic conditions (12.8 g, Sigma-Aldrich, 98%) was added to the solution, stirring continued for 20 h. Then, the mixture was aged at 90 °C in a Teflon bottle for 24h under static conditions. The resulting white powder was obtained by filtration and purified via washing with ethanol and deionized water. The purified product was calcined at 550 °C for 12h using a heating ramp rate 2 °C/min. [25].

All the SBA-15 samples (Na-SBA-15, NaOH-SBA-15, and Li-SBA-15 and LiOH-SBA-15) were metal-loaded by the method of incipient wetness impregnation (IWI) with Na₂CO₃ as a sodium precursor, Li₂CO₃ as a lithium precursor, LiOH as a lithium hydroxide precursor and NaOH as a sodium hydroxide precursor. Impregnation solutions were prepared by dissolving the appropriate amount of metals (2% loading) is introduced into H₂O solvent to load the catalyst with a total of 2wt%. In order to

achieve a high metal dispersion and inhibit agglomeration of the salt during the vaporization of the solvent, the total volume of the solution was equal to that of the used pore volume of the support. After impregnation, the catalysts were dried overnight in air at ambient temperature, then 24 h at 120 °C, and finally calcined at 500 °C for 4 h to get the 2%Na/SBA-15, 2% NaOH/SBA-15, 2% Li/SBA-15 and 2%LiOH-SBA-15 catalysts.

Characterization

The small-angle XRD patterns were recorded under ambient conditions on MiniFlex (Rigaku) XRD with Cu K α radiation ($\lambda = 1.5406\text{\AA}$). The X-ray tube was operated at 40 kV and 30 mA while the diffractometer were recorded in the 2θ range of $0.5\text{--}8^\circ$ with a 2θ step size of 0.01 and a step time of 10s. The d-spacing and unit cell parameters were calculated using the corresponding formulas, $n\lambda = 2d\sin\theta$ and $a_0 = 2d100/\sqrt{3}$.

Nitrogen adsorption/desorption measurements were conducted using a Micromeritics ASAP 2020 pore analyzer by N₂ physisorption at -196°C. All samples were degassed for 3 h at 350 °C under vacuum ($p < 10^{-5}$ mbar) in the degas port of the sorption analyzer. The BET specific surface areas of the samples were calculated using Brunauer–Emmett–Teller (BET) method in the range of relative pressures between 0.05 and 0.35. The pore size distributions were calculated from the adsorption branch of the isotherm using the thermodynamics-based Barrett–Joyner–Halenda (BJH) method. The total pore volume was determined from the adsorption branch of the N₂ isotherm as the amount of liquid nitrogen adsorbed at $P/P_0 = 0.995$. The pore wall thickness (t_w) was calculated from unit cell parameter (a_0) and pore size diameter (d_p). Mean mesopore diameters for the various samples were estimated from the nitrogen sorption data using BET analysis ($4V/A$). The macro pore structure was characterized by scanning electron microscopy (SEM), performed on a JEOL (JSM-5600 LV) scanning electron microscope. EDAX used in combination with SEM is an analytical technique which forms an elemental analysis of the catalyst to identify the chemical composition.

The infrared spectra (FT- IR) of the solid samples diluted in (8 wt %) KBr were recorded at room temperature in transmission mode in the range of 4000 to 400 cm^{-1} at 4 cm^{-1} resolution regions using NICOLET 380 FT-IR spectrometer.

Catalytic activity reactions

The transesterification of vegetable oil was carried out in a four stirred glass reactor 500 ml which was used for the transesterification of vegetable oil to biodiesel which equipped with a reflux condenser, which was placed in a thermostatic bath with a magnetic stirrer. The stirred glass reactor was kept in an oil bath. Esterification reaction was performed under atmospheric pressure after that reaction procedure was as follows. The condenser generally served to return the evaporated methanol back to the reactor vessel. 80 ml of vegetable oil and 20 ml of methanol (molar ratio of methanol to vegetable oil 6:1) were added into the glass reactor with 1 g of catalyst, and then the temperature was raised to 65 °C under stirring for 4 h. the calculated amount of catalyst was dispersed in the methanol under stirring. Then, vegetable oil was added into the mixture and the temperature was set to the desired value with suitable stirring rate. After reaching the desired reaction time, the mixture was taken out and excess methanol was distilled off under vacuum. The biodiesel was isolated by decantation in a separating funnel, allowing the glycerol to separate from the methyl ester by gravity for 5 h. Then the catalyst was separated by centrifugation.

After removing the glycerol layer as mentioned above, the biodiesel layer was collected for chromatographic analysis. The biodiesel yield was calculated from the methyl ester and vegetable oil weights. The physical properties and chemical composition of biodiesel were tested according to the ASTM D975T test method.

Analytical methods

Reference materials and product samples were analyzed using a (GC) type (5890 series II gas chromatograph) equipped with a capillary column (Nucol, 50 m × 50 μm) and a flame ionization detector (FID). Helium was used as the carrier gas. The injector temperature was kept at 220 °C and the detector temperature was set at 250 °C. The analysis of biodiesel for each reaction mixture was carried out by dissolving 100 μl of diluted sample (biodiesel sample in n-hexane) into 100 μl of internal standards solution (concentration = 1 g/l). Then, 1 μl of this mixture was injected into the GC.

RESULT AND DISCUSSION

Characterization of the synthesized materials

The XRD patterns of SBA-15 samples before and after modification Figure (2) all displayed an intense diffraction peak at about 2θ of 0.9° , which is characteristic of a mesostructure. Moreover, two additional peaks were observed in the XRD patterns, which can be indexed as (1 1 0) and (2 0 0) reflections of a hexagonal P6mm symmetry [26]. The results demonstrate that the periodic ordered structure of SBA-15 was maintained after modification. However, spacing values (a_0) of the grafted SBA-15 samples reduced somewhat see Table (1), compared to SBA-15, indicating changes in their wall thickness and pore size due to the deposition of loaded alkaline metals and its hydroxides. The nitrogen adsorption isotherms of SBA-15 and four grafted SBA-15 materials had similar patterns as a type IV isotherm and a hysteresis loop type H1 Figure (3); hysteresis loops with sharp adsorption and desorption branches are indicative of a narrow pore size distribution. Figure (3) also shows that the nitrogen adsorbed amount decreases as SBA-15 is grafted with loaded alkaline metals and alkali metal hydroxides. The structural parameters calculated from nitrogen adsorption measurements are presented in Table (1). In the table, it is shown that the specific surface area, pore volume, and pore size of the samples followed the order: SBA-15 > 2%Li/SBA-15 > 2%NaOH/SBA-15 > 2% Na/SBA-15 and 2% LiOH/SBA-15 whereas the different order was observed in terms of wall thickness.

The significant decreases in the surface area of the loaded samples in comparison with SBA-15 confirm the attaching of supported metals groups inside the pores [26-28].

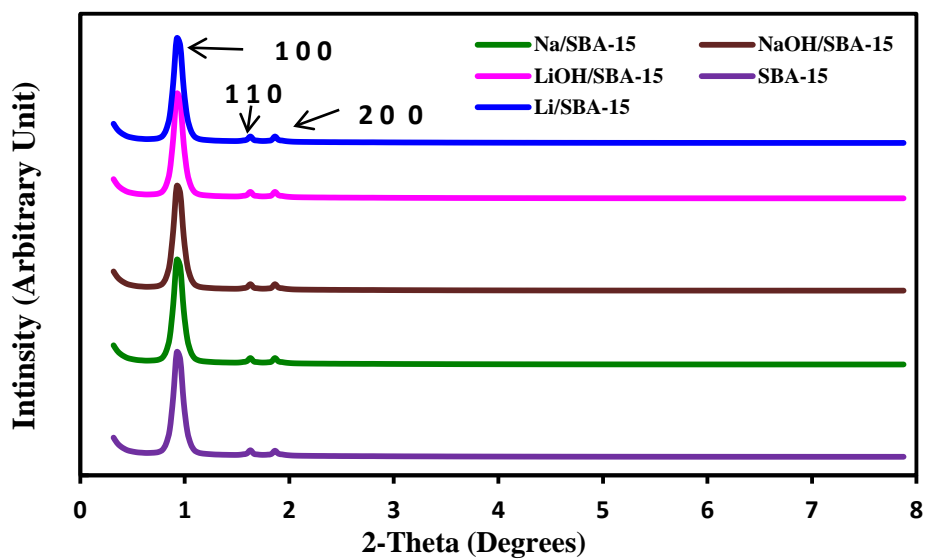


Figure (2) X-ray diffraction patterns of (SBA-15) and supported Alkali Metals and alkali metal hydroxides catalysts.

Table (1) Physicochemical properties of SBA-15 materials and with different Alkali metals and alkali metal hydroxides loaded used in catalysis tests.

Sample	S_{BET} (m^2/g)	V_P (cm^3/g)	$V_{\mu P}$ (cm^3/g)	D_P (nm)	α_o (nm)	t_{wall} (nm)
SBA-15	900	1.88	0.07	8.5	11.08	2.58
Na/ SBA-15	735	1.09	0.08	6.05	10.62	4.57
NaOH/ SBA-15	780	1.17	0.08	6.16	10.29	4.13
Li/SBA-15)	791	1.25	0.07	7.86	10.84	2.98
LiOH/SBA-15	775	1.13	0.07	7.37	10.23	3.15

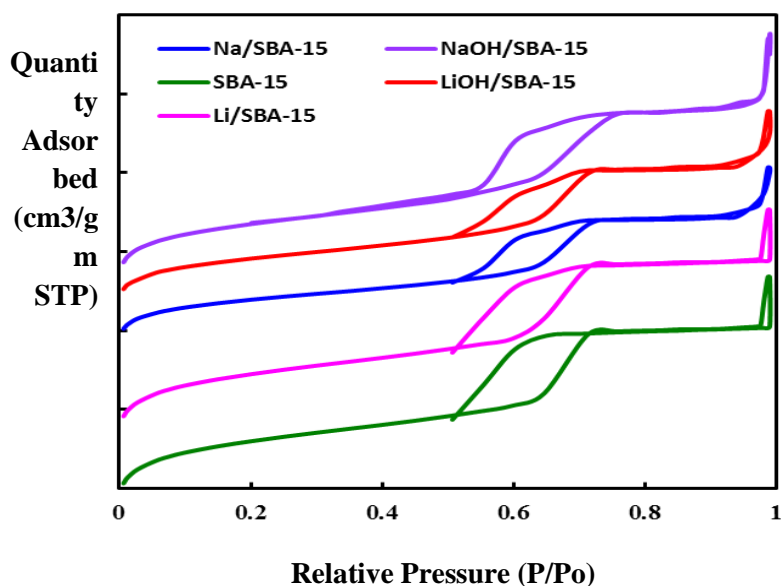


Figure (3) Nitrogen adsorption isotherms for SBA-15, 2% Na/SBA-15, 2%NaOH/SBA-15, 2%Li/SBA-15 and 2%LiOH/SBA-15 samples.

SEM and EDAX of catalysts

SEM and EDAX characterisation techniques were performed on the prepared catalyst samples prior to testing. SEM images of SBA-15 can be seen in Figure (4) at magnifications of 10,000. The surface morphology SBA-15 sample is very similar. However the SBA-15 particles are much smaller.

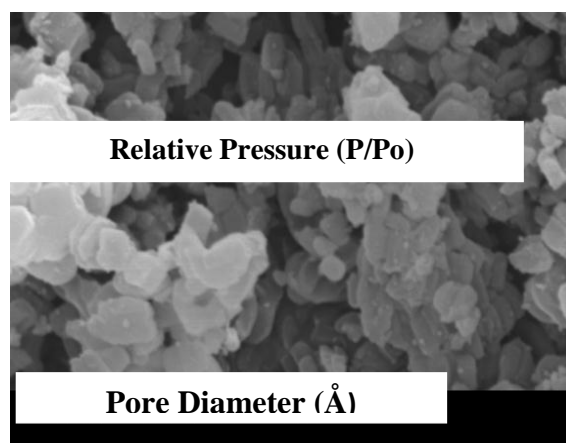


Figure (4) SEM image of SBA-15 at a magnification of 10,000.

EDAX was performed on the tested catalyst samples. Typical EDAX images for SBA-15 can be seen in Figure (5). The peaks from the EDAX graph resulting from the SBA-15 catalyst indicated the zeolite was composed of C, O, Si and Al. EDAX

graphs were generated for several different points on the SEM images in order to gain correct average wt% values for each of the components. Therefore the error in these results can be assumed to be minimal. The Si average weight percent of SBA-15 was found to be 40.96 wt % from the EDAX images.

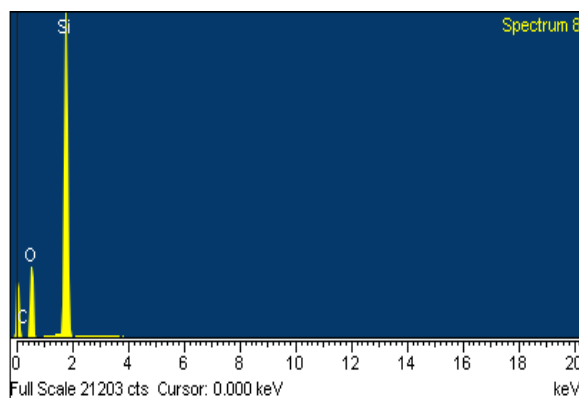


Figure (5) Typical EDAX image for SBA-15.

Figure (6) shows the FT-IR spectra of SBA-15 and the various catalysts. The spectra of all the materials contain the typical Si–O–Si bands around 1078, 804 and 455 cm^{-1} , which arise from the Si O Si stretching vibration. The absorption band at around 960 cm^{-1} can be assigned to either Si OH or Si O Si stretching vibrations. The broad band at around 3400 cm^{-1} is due to the presence of surface OH groups with strong H-bonding interactions between them. Finally the band at around 1631 cm^{-1} can be assigned to the deformation modes of OH bonds of adsorbed H_2O [29]. A loaded Alkali metals and alkali metal hydroxide sample exhibits a very similar spectrum to SBA-15 due to its low metals and hydroxide content, whereas all catalysts with 2% Na/SBA-15, 2% NaOH/SBA-15, 2% Li/SBA-15 and 2% LiOH/SBA-15 exhibits two additional bands at 660 and 570 cm^{-1} (black arrows) [30-32]. The modified Alkali metals and alkali metal hydroxides on SBA-15 bands are slightly more intense than for SBA-15. As the metals content is the same for both catalysts, we attribute this to the presence of larger Particles on the external surface of the pores for all above samples also exhibit the same absorbance bands, with progressively increasing intensity [32]. The results demonstrate that the amount of Si–OH groups was utilized most in 2% LiOH/SBA-15, 2% Na/SBA-15, NaOH/SBA-15 and Li/SBA-15 respectively, which is consistent with the surface coverage of these materials, see Table (1).

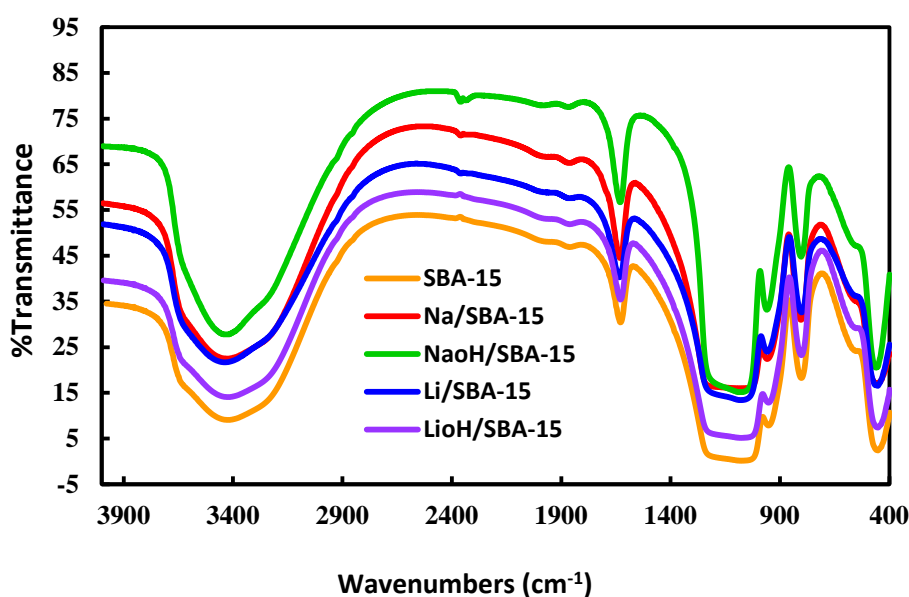


Figure (6) FT-IR spectra of SBA-15 and all alkali metals and alkali metal hydroxides catalysts.

Esterification reactions

After separation and purification process, the physical properties and chemical composition of biodiesel were tested according to the ASTM D975T method. Table 2 shows some of the most important physical properties of four different reaction products, where the methyl esters analyzed through GC for each catalytic heterogeneous reaction by alkali metal (or alkaline earth metal) and alkali metal hydroxides encapsulated nanoporous material SBA-15 catalysts. In this table, it can be observed that all samples of biodiesel synthesized via acid heterogeneous catalysis had quality properties very close to conventional fossil diesel. The values of density, cloud point, acid value and iodine value (I) for the reaction products are consistent with the composition of the samples. For example, the API gravity of most of the reaction products was very close to 31° API, which corresponds to the boundary between medium and heavy crude. The FFAs content, expressed as mg of KOH required to neutralize the free fatty acids in 1 g of oil (acid number), was determined according to the standard ASTM D 975T procedure; an acid number of (0.274-0.206) Mikohn/goil respectively as in Table (2) was obtained. Average molar masses of 296.32 g/mole were calculated and measured by mass spectra instrument for the methyl esters products, which were obtained from the esterification of vegetable oil to biodiesel.

Table (2) Physical properties of the biodiesels products.

Type of catalyst	°API	Density (g/cm ³) of biodiesels	Cloud Point	Acid Value (mgKOH/g)	Iodine Value (I) g/100g FAME
Na/SBA-15	25.8	0.8994	-9 °C	0.274	109.43
NaOH/SBA-15	31.2	0.8694	-6 °C	0.234	112.72
Li/SBA-15	30.8	0.8714	-6 °C	0.256	122.77
LiOH/SB-15	30.9	0.8712	-2 °C	0.206	123.79

The catalytic activities of the heterogeneous catalysts which having different amounts of loaded alkali metal and alkali metal hydroxides supported catalysts on SBA-15 were measured, the biodiesel conversion (wt %) was measured and presented for each catalyst all are presented in Figure (7) which shows the histogram conversion for each reaction, which was calculated from the amount of fatty acids remaining in each product, as compared to the amount of fatty acids present in the initial reactant. All the base catalysts had good catalytic activity with conversions around (85-94%) except for Na/SBA-15 showed the worst activity, with a yield of around 70wt%. which could be attributed to a decrease in the surface area of the SBA-15 metals that were loading.

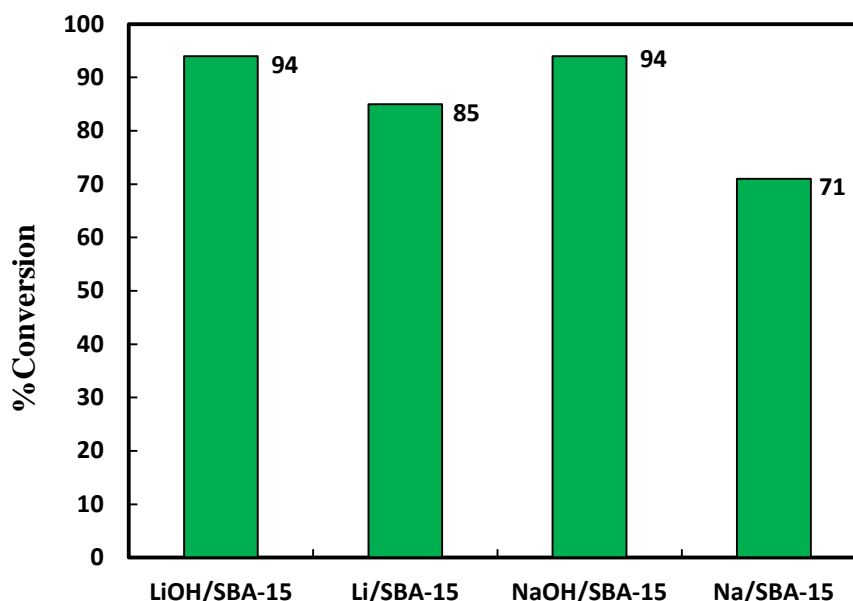


Figure (7) Conversion percentages for esterification reaction of green oil to biodiesel using different base catalyst. The Molar ratio Methanol/oil was 6:1 (T = 65°C, 4 h).

CONCLUSIONS

1. Catalysts with alkali metal and alkali metal hydroxides linked to SBA-15 surface Have been successfully prepared and characterized.
2. The Nano structural parameters obtained by Characterization of the synthesized materials analyses are very similar for all samples evidencing that the impregnation method for incorporation of alkali metal and alkali metal hydroxides in mesoporous silica does not affect its structure.
3. Heterogeneous base catalysts take advantages of the easy recovering from the reaction medium, and thus they can be reused as such or after regeneration.
4. All the heterogeneous catalysts showed conversions above 70%.
5. The physical properties and chemical composition of the biodiesel product were better than conventional fossil diesel.
6. This study shows that the mesoporous SBA-15 based catalyst has proven to be a promising one for the transesterification of vegetable oil with methanol.

Acknowledgements

Dr. Talib M. Albeit is grateful to the University of Technology, in Republic of Iraq, for allowing postdoctoral leave and to Manchester Metropolitan University, in British United Kingdom (UK), for financial support.

REFERENCES

- [1]. Leckel D., Diesel Production from Fischer-Tropsch: The Past, the Presence and New Concepts, *Energy & Fuels* 23 (2009) (2342-2358).
- [2]. George W. Huber, Sara Ibarra, and Avelino Corma, Synthesis of Transportation Fuels from Biomass: Chemistry, Catalysts, and Engineering, *Chem. Rev.*, 106 (2006)4044–4098.
- [3]. Zhang Y. H., Reviving the carbohydrate economy via multi-product lignocellulose biorefineries, *J. Ind. Microbiol. Biotechnol.*, 35(2008) 367–375.
- [4]. Alonso, D.M.; Bond, J.Q.; Dumesic, J.A.; Catalytic conversion of biomass to biofuels. *Green Chemistry*. 12 (2010) 1493-1513.
- [5]. Xiaoyuan Liao, Yulei Zhu, Sheng-Guang Wang, Yongwang Li, Producing triacetyl glycerol with glycerol by two steps: Esterification and acetylation, *Fuel Processing Technology* 90 (2009) 988–993.
- [6]. Lopez Granados, M. A.C. Alba-Rubio, F. Vila, D. Martin Alonso, R. Mariscal, Surface chemical promotion of Ca oxide catalysts in biodiesel production reaction by the addition of monoglycerides, diglycerides and glycerol, *Journal of Catalysis* 276 (2010) 229–236.
- [7]. Ana C. Alba-Rubio, F. Vila, D. Martin Alonso, M. Ojeda, R. Mariscal, M. Lopez Granados, "Deactivation of organosulfonic acid functionalized silica catalysts during biodiesel synthesis", *Applied Catalysis B: Environmental* 95 (2010) 279-287.
- [8]. Valter L.C. Gonçalves, Bianca P. Pinto, João C. Silva, Claudio J.A. Mota, Acetylation of glycerol catalyzed by different solid acids, *Catalysis Today* 133–135 (2008) 673–677.
- [9]. Bernhard M.E. Russbuehdt, Wolfgang F. Hoelderich, New rare earth oxide catalysts for the transesterification of triglycerides with methanol resulting in biodiesel and pure glycerol, *Journal of Catalysis* 271 (2010) 290–304.

- [10]. Meher LC, Sagar DV, Naik SN. Technical aspects of biodiesel production by transesterification: a review. *Renew Sustain Energy Rev* 2006; 10:248–68.
- [11]. Boey PL, Maniam GP, Hamid SA. Biodiesel production via transesterification of palm olein using waste mud crab (*Scylla serrata*) shell as a heterogeneous catalyst. *Bioresource Technology* 2009; 100:6362–8.
- [12]. Umdu ES, Tuncer M, Seker E. Transesterification of nanochloropsis microalgae lipid biodiesel on Al_2O_3 supported CaO and MgO catalysts. *Bioresource Technology* 2009; 100:2828–31.
- [13]. Xie W, Huang X, Li H. Soybean oil methyl esters preparation using NaX zeolites loaded with KOH as a heterogeneous catalyst. *Bioresource Technology* 2007; 98:936–9.
- [14]. A.E. Barron Cruz, J.A. Melo Banda, Hernandez Mendoza, C.E. Ramos-Galvan, M.A. MerazMelo, Dominguez Esquivel. Pt and Ni supported catalysts on SBA-15 and SBA-16 for the synthesis of biodiesel. *Catalysis Today* 166 (2011) 111–115.
- [15]. Wang Y, Wang X, Liu Y, Ou S, Tan Y, Tang S. Refining of biodiesel by ceramic membrane separation. *Fuel Process Technology* 90 (2009) 422–427.
- [16]. Helwani Z, Othman MR, Aziz N, Kim J, Fernando WJN. Solid heterogeneous catalysts for transesterification of triglycerides with methanol: a review. *Appl Catal A: Gen* 2009; 363:1–10.
- [17]. Zabeti M, Wan M, Wan D. Activity of solid catalysts for biodiesel production: a review. *Fuel Process Technol* 2009; 90:770–7.
- [18]. Sarma AK, Sarmah JK, Barborá L, Kalita P, Chatterjee S, Mahanta P, et al. Recent inventions in biodiesel production and processing: a review. *Recent Patent Eng* 2008; 2:47–58.
- [19]. Lee JS, Saka S. Biodiesel production by heterogeneous catalysts and supercritical technologies: review. *Bioresource Technology* 2010; 101:7191–200.
- [20]. Canakci M, Van Gerpan J. Biodiesel production from oils and fats with high free fatty acids. *Trans ASAE* 2001; 44:1429–36.
- [21]. Grandos ML, Poves MD, Alonso D, Mariscal R, Galisteo FC, Moreno-Tost R, et al. Biodiesel from sunflower oil by using activated calcium oxide. *Appl Catal B: Environ* 2007; 73:317–26.
- [22]. Ji J, Wang J, Li Y, Yu Y, Xu Z. Preparation of biodiesel with the help of ultrasonic and hydrodynamic cavitation. *Ultrasonic* 2006; 44:4114.
- [23]. Kumar KS, Anju C. Preparation of biodiesel from crude oil of *Pongamia pinnata*. *Bioresource Technology* 2005; 96:1425–9.
- [24]. Dongyuan Zhao, Qisheng Huo, Jianglin Feng, Bradley F. Chmelka and Galen D. Stucky, (1998). *Journal American Chemical Society*, 120, 6024.
- [25]. John N. Kuhn, Wenyu Huang, Chia-Kuang Tsung, Yawen Zhang, and Gabor A. Somorjai, (2008). *Journal American Chemical Society*, 130, 14026-14027.
- [26]. D. Zhao, J. Feng, Q. Huo, N. Melosh, G.H. Fredrickson, B.F. Chmelka, G.D. Stucky, Triblock copolymer syntheses of mesoporous silica with periodic 50–300 angstrom pores, *Science* 279 (1998) 548–552.
- [27]. Kruk, M. M. Jaroniec, A. Sayari, *Chem. Mater.* 11 (1999) 492–500.
- [28]. Jamileh Taghavimoghaddam, Gregory P. Knowles, Alan L. Chaffee. Preparation and characterization of mesoporous silica supported cobalt oxide as a catalyst for the oxidation of cyclohexanol, *Journal of Molecular Catalysis A: Chemical* 358 (2012) 79–88.

- [29]. Chiu, J. J., Pine, D. J., Bishop, S. T., Chmelka, B. F. Friedel–Crafts alkylation properties of aluminosilica SBA-15 meso/macro porous monoliths and mesoporous powders, *Journal of Catalysis*, 221 (2004) 400-412.
- [30]. Tanya Tsoncheva, Ljubomir Ivanova, Christo Minchev, Michael Fröba, Cobalt-modified mesoporous MgO, ZrO₂, and CeO₂ oxides as catalysts for methanol decomposition, *Journal of Colloid and Interface Science* 333 (2009) 277–284.
- [31]. Lipeng Zhou, Jie Xu, Hong Miao, Feng Wang, Xiaoqiang Li, Catalytic oxidation of cyclohexane to cyclohexanol and cyclohexanone over Co₃O₄ nanocrystals with molecular oxygen, *Applied Catalysis A: General* 292 (2005) 223–228.
- [32]. Lin, L. Ji, J. H.C. Zeng, “Metal-support interactions in Co/Al₂O₃ catalysts: a comparative study on reactivity of support,” *Journal of Physical Chemistry B*, 104 (2000) 1783–1790.